Structural and Multidisciplinary Optimization manuscript No.
(will be inserted by the editor)

Robust Design Optimization with Design-Dependent Random Input Variables

Benedikt Kriegesmann

Received: date / Accepted: date

Abstract This paper addresses the dependency of design parameters and random variables within robust design optimization. If the stochastic distributions of random input variables are design-dependent, then this dependency must be included in the gradient, when using gradient-based optimization methods. The paper provides the basic theoretical principles and two approaches for incorporating design-dependent distributions of random variables in robust design optimization: one approach based on Monte Carlo sampling and another based on Taylor series expansions. Both these approaches do not require additional structural analyses (e.g. finite element simulations). Describing the design dependency of input distributions can, however, be a challenging task. Numerical applications to different academic examples are presented, demonstrating the potential of the proposed approaches and several implications that may emerge in the process.

Keywords robust design optimization · design-dependent random variables · robust topology optimization · probabilistic approaches

1 Introduction

Deterministic optimization of structures involves the risk of providing designs that are very sensitive to the deviations of nominal configurations (for instance load, geometry, material properties, ...). Robust design optimization (RDO) approaches take into account the variability of random input variables and derive a design that is less sensitive to variations (see, e.g., [16, 25, 15]). For an overview of RDO methods, the reader is referred to [19] and [27]. Typical input parameters, which are subject to scatter, are material properties, load orientation and magnitude as well as geometric measures. For certain problems, the stochastic distribution of random input parameters may be dependent on the design parameters. One example of this is the geometric imperfection of a cylindrical shell, which heavily influences the load carrying capability and is, at the same time, dependent on the design (see, e.g., [1, 2]). Further examples include the build stress and distortion in additively manufactured metal parts, which are dependent on the design and the support structure (see, e.g., [11]), or in composite structures where build stress and distortion are influenced by the shape and the laminate stacking sequence [17]. The dependency of the input distribution on the design parameters can be determined by probabilistic manufacturing simulations, which is a challenging task on its own and beyond the scope of this paper.

When using non-gradient based optimization approaches like genetic algorithms (as, e.g., in [25]), the distribution of input variables can be updated for each function evaluation. However, they are not appropriate for solving optimization tasks with a large number of design parameters such as topology optimization [28].

When using gradient based optimization algorithms, the change of the distribution of input parameters needs to be included in the gradient of the optimization objective in order to ensure convergence. Cho et al [5] considered standard deviations and correlations of input variables as design dependent. They derived the derivatives of the probability of failure given by approximations at the most probable point in the framework of reliability-based design optimization. A dependency of the complete probability density function can be addressed by the score function method [24]. It provides

B. Kriegesmann
Hamburg University of Technology
E-mail: benedikt.kriegesmann@tuhh.de

the derivatives of an expected performance with respect to varying parameters of the random distribution. The limitation of this method is that the objective function must not be dependent on these parameters [21]. To the best of the author's knowledge, a dependency of both the objective function and the complete probability density function on design parameters of a robust design optimization has not been addressed, yet.

In this paper, the basic theory is presented for considering the design dependency of random variables in the gradient of RDO problems. Two possible ways to determine the gradient are shown, one based on Monte Carlo sampling and one based on a Taylor series expansion of the objective function. Subsequently, the presented approaches are applied to simple examples of structural analysis. When considering compliance as objective function, all derivatives are given which are required for the gradient determination when using finite element analyses. The derivatives of typical stochastic distributions are also given in the context of the examples.

2 Robust design gradients considering design-dependent random variables

Consider a probabilistic objective function $g(\mathbf{x},\mathbf{y})$ which is a function of the random vector $\mathbf{X}$ with probability density function (PDF) $f_{\mathbf{X}}(\mathbf{x},\mathbf{y})$, and the set of design parameters $\mathbf{y}$. Note that we allow the PDF of $\mathbf{X}$ to be a function of the design parameters $\mathbf{y}$. Examples for random parameters are the Young's modulus, the geometry or the applied load. Typical design parameters are geometry parameters, the layup of a composite or the density distribution in topology optimization. Random parameters and design parameter may refer to the same physical property, which is discussed in detail in the context of an example in Section 3.3.

The robust design optimization problem considered is given by

$$\begin{aligned} &\min_{\mathbf{y}} \mu_g(\mathbf{y}) + \kappa\, \sigma_g(\mathbf{y}) \\ &\text{subject to } \ \mathbf{c}_{neq}(\mathbf{y}) \leq 0 \\ &\qquad\qquad\ \ \mathbf{c}_{eq}(\mathbf{y}) = 0 \end{aligned} \tag{1}$$

Here, $\mathbf{c}_{neq}(\mathbf{y})$ is a vector of inequality constraints, and $\mathbf{c}_{eq}(\mathbf{y})$ is a vector of equality constraint functions. The scalar κ weighs the standard deviation σ_g, with respect to the mean μ_g. The constraints may also include probabilistic measures, for instance a maximum probability of failure or a maximum variance. They should however not directly depend on random parameters in order to ensure that they are fulfilled[1].

This sections deals with the derivation of the gradient of the objective function, i.e. the gradient of mean value and variance, if the PDF is a function of the design parameters $\mathbf{y}$.

Other sources use different weight factors [6] and/or combine different objective functions (e.g. volume and variance of strength [34]) and/or use the variance instead of the standard deviation [32]. In any case, the gradient of the mean and/or variance of the different function(s) are required for the optimization.

2.1 General formulation

The gradient of the optimization objective (1) can be written as

$$\frac{\partial \mu_g}{\partial y_k} + \kappa \frac{\partial \sigma_g}{\partial y_k} = \frac{\partial \mu_g}{\partial y_k} + \kappa \frac{1}{2\sigma_g} \frac{\partial \sigma_g^2}{\partial y_k}$$

Hence, the derivatives of the mean μ_g and the variance σ_g^2 of the probabilistic objective function $g(\mathbf{x},\mathbf{y})$ are required. The stochastic moments themselves are given by

$$\mu_g(\mathbf{y}) = \int_{-\infty}^{\infty} g(\mathbf{x},\mathbf{y}) f_{\mathbf{X}}(\mathbf{x},\mathbf{y}) d\mathbf{x} \tag{2}$$

and

$$\begin{aligned} \sigma_g^2(\mathbf{y}) &= \int_{-\infty}^{\infty} \left[g(\mathbf{x},\mathbf{y}) - \mu_g\right]^2 f_{\mathbf{X}}(\mathbf{x},\mathbf{y}) d\mathbf{x} \\ &= \int_{-\infty}^{\infty} g^2(\mathbf{x},\mathbf{y}) f_{\mathbf{X}}(\mathbf{x},\mathbf{y}) d\mathbf{x} - \mu_g^2 \end{aligned} \tag{3}$$

The derivative of the mean with respect to a design variable y_k reads

$$\begin{aligned} \frac{\partial \mu_g(\mathbf{y})}{\partial y_k} &= \int_{-\infty}^{\infty} \frac{\partial g(\mathbf{x},\mathbf{y})}{\partial y_k} f_{\mathbf{X}}(\mathbf{x},\mathbf{y}) d\mathbf{x} \\ &\quad + \int_{-\infty}^{\infty} g(\mathbf{x},\mathbf{y}) \frac{\partial f_{\mathbf{X}}(\mathbf{x},\mathbf{y})}{\partial y_k} d\mathbf{x} \end{aligned} \tag{4}$$

[1] For instance, when the cross sections of bars are considered as design variables *and* random parameters, a volume constraint should be evaluated with design variables and not with the random component, see also Section 3.3.

The derivative of the variance equals

$$\frac{\partial \sigma_g^2(\mathbf{y})}{\partial y_k} = \int_{-\infty}^{\infty} 2g(\mathbf{x},\mathbf{y}) \frac{\partial g(\mathbf{x},\mathbf{y})}{\partial y_k} f_{\mathbf{X}}(\mathbf{x},\mathbf{y}) d\mathbf{x} + \int_{-\infty}^{\infty} g^2(\mathbf{x},\mathbf{y}) \frac{\partial f_{\mathbf{X}}(\mathbf{x},\mathbf{y})}{\partial y_k} d\mathbf{x} - 2\mu_g \frac{\partial \mu_g(\mathbf{y})}{\partial y_k} \tag{5}$$

The second summands in Eq. (4) and (5) only occur if the distribution of $\mathbf{X}$ is dependent on $\mathbf{y}$ and therefore do not occur in existing RDO approaches. In contrast, the score function method only considers these summands.

2.1.1 Piecewise-defined stochastic distributions

Some common stochastic distributions are defined piecewise and/or within certain bounds, for instance uniform, Simpson, and Beta distribution. Then, the integrals in Eq. (2) to (5) are solved piecewise, where the integral bounds can be dependent on the design parameters. To exemplify this, consider a one-dimensional case with one design parameter y and one random variable X, which is bounded by $l(y)$ and $u(y)$ (i.e., $f_X = 0$ for $x < l(y)$ and $x > u(y)$). The mean value of an objective function g is then given by

$$\mu_g(y) = \int_{l(y)}^{u(y)} g(x,y) f_X(x,y) dx$$

Since the integration bounds are dependent on the design variable y, the derivative of μ_g, with respect to y, requires applying the Leibniz integral rule [20]; this yields

$$\begin{aligned}\frac{\partial \mu_g(y)}{\partial y} = &\int_{l(y)}^{u(y)} \frac{\partial g(x,y)}{\partial y} f_X(x,y) dx \\ &+ \int_{l(y)}^{u(y)} g(x,y) \frac{\partial f_X(x,y)}{\partial y} dx \\ &+ g(u(y),y) f_X(u(y),y) \frac{\partial u(y)}{\partial y} \\ &- g(l(y),y) f_X(l(y),y) \frac{\partial l(y)}{\partial y}\end{aligned}$$

For a multi-variate distributed random vector $\mathbf{X}$, for which the PDF is non-zero in the domain Ω, the Leibniz integral rule yields

$$\frac{\partial}{\partial y_k} \int_{\Omega} g(\mathbf{x},\mathbf{y}) f_{\mathbf{X}}(\mathbf{x},\mathbf{y}) d\mathbf{x} = \int_{\Omega} \frac{\partial g(\mathbf{x},\mathbf{y})}{\partial y_k} f_{\mathbf{X}}(\mathbf{x},\mathbf{y}) d\mathbf{x} + \int_{\Omega} g(\mathbf{x},\mathbf{y}) \frac{\partial f_{\mathbf{X}}(\mathbf{x},\mathbf{y})}{\partial y_k} d\mathbf{x} + \oint_{\Gamma} g(\mathbf{x},\mathbf{y}) f_{\mathbf{X}}(\mathbf{x},\mathbf{y}) \mathbf{v}_b \mathbf{n} dS$$

Here, the last summand is an integral over the boundary Γ of the domain, $\mathbf{n}$ is a normal vector on the (hyper) surface element dS, and $\mathbf{v}_b$ is the gradient of the boundary with respect to the design vector $\mathbf{y}$. The integral over the boundary may become very complex in higher dimensions and/or for correlated parameters. Alternatively, the piecewise distribution can be approximated by a continuous function; this allows the gradients to be determined as given in Eq. (4) to (5). Both possibilities are described in detail for the example in Section 3.3.

2.2 Monte Carlo approximation

The mean value and variance as well as their derivatives can be approximated by the Monte Carlo method (for details on the Monte Carlo method, refer to textbooks such as [8]). Using a simple sampling approach, where realizations $\mathbf{x}^{(i)}$ of $\mathbf{X}$ are generated based on the probability density $f_{\mathbf{X}}$, mean value and variance are estimated from

$$\mu_g(\mathbf{y}) \approx \frac{1}{m} \sum_{i=1}^{m} g(\mathbf{x}^{(i)},\mathbf{y}) \tag{6}$$

and

$$\sigma_g^2(\mathbf{y}) \approx \frac{1}{m-1} \sum_{i=1}^{m} g^2(\mathbf{x}^{(i)}) - \mu_g^2 \tag{7}$$

Here, m is the number of realizations. The efficiency can be improved by using importance sampling, for instance.

The first summands of the derivatives of mean (4) and variance (5) can also be approximated with the Monte Carlo method. The second summands, however, include the derivative of the PDF, with respect to design variables. This derivative is not a PDF; it is, in general, not strictly positive and the integral over its domain is not equal to 1. In order to allow the same sampling approach for these terms, the function $\boldsymbol{\varphi}$ is introduced.

$$\begin{aligned}&\boldsymbol{\varphi}(\mathbf{x},\mathbf{y}) = \frac{\frac{\partial f_{\mathbf{X}}(\mathbf{x},\mathbf{y})}{\partial y}}{f_{\mathbf{X}}(\mathbf{x},\mathbf{y})} \\ \Leftrightarrow \quad &\frac{\partial f_{\mathbf{X}}(\mathbf{x},\mathbf{y})}{\partial y} = f_{\mathbf{X}}(\mathbf{x},\mathbf{y}) \varphi(\mathbf{x},\mathbf{y})\end{aligned} \tag{8}$$

In the framework of the score function method, $\boldsymbol{\varphi}$ is referred to as the efficient score function [24]. For bounded random distributions like uniform, Beta or Weibull distribution, $f_{\mathbf{X}}(\mathbf{x},\mathbf{y}) = 0$ outside of these bounds. Hence, outside the bounds $\boldsymbol{\varphi}$ is undefined. However, this has no practical impact on the Monte Carlo simulation, since samples are generated only inside the bounds of a distribution.

With (8), Eq. (4) and (5) can be written as

$$\frac{\partial \mu_g(\mathbf{y})}{\partial y_k} = \int_{-\infty}^{\infty} \left[\frac{\partial g(\mathbf{x},\mathbf{y})}{\partial y_k} + g(\mathbf{x},\mathbf{y})\, \boldsymbol{\varphi}(\mathbf{x},\mathbf{y}) \right] f_{\mathbf{X}}(\mathbf{x},\mathbf{y})\, d\mathbf{x} \tag{9}$$

and

$$\begin{aligned} \frac{\partial \sigma_g^2(\mathbf{y})}{\partial y_k} = \int_{-\infty}^{\infty} \Big[& 2g(\mathbf{x},\mathbf{y}) \frac{\partial g(\mathbf{x},\mathbf{y})}{\partial y_k} \\ & + g^2(\mathbf{x},\mathbf{y})\, \boldsymbol{\varphi}(\mathbf{x},\mathbf{y}) \Big] f_{\mathbf{X}}(\mathbf{x},\mathbf{y})\, d\mathbf{x} - 2\mu_g \frac{\partial \mu_g(\mathbf{y})}{\partial y_k} \end{aligned} \tag{10}$$

Eq. (9) and (10) can be solved with the Monte Carlo method similarly as follows.

$$\frac{\partial \mu_g(\mathbf{y})}{\partial y_k} \approx \frac{1}{m} \sum_{i=1}^{m} \left[\frac{\partial g\left(\mathbf{x}^{(i)},\mathbf{y}\right)}{\partial y_k} + g\left(\mathbf{x}^{(i)},\mathbf{y}\right) \varphi\left(\mathbf{x}^{(i)},\mathbf{y}\right) \right] \tag{11}$$

$$\begin{aligned} \frac{\partial \sigma_g^2(\mathbf{y})}{\partial y_k} \approx \frac{1}{m} \sum_{i=1}^{m} \Big[& 2g\left(\mathbf{x}^{(i)},\mathbf{y}\right) \frac{\partial g\left(\mathbf{x}^{(i)},\mathbf{y}\right)}{\partial y_k} \\ & + g^2\left(\mathbf{x}^{(i)},\mathbf{y}\right) \varphi\left(\mathbf{x}^{(i)},\mathbf{y}\right) \Big] - 2\mu_g \frac{\partial \mu_g(\mathbf{y})}{\partial y_k} \end{aligned} \tag{12}$$

Note that by introduction of the score function $\boldsymbol{\varphi}$ the same realizations are used for the evaluation of all terms of eqs. (6), (7), (11) and (12). This does not hold anymore in case the bounds of the input distribution are design-dependent, as discussed in Section 2.1.1. Then, the Monte Carlo approach needs to be modified to solve the integral over the domain boundary. This means that new samples have to be generated, which are located on the boundary, and for these samples the objective function needs to be evaluated. This causes significant additional effort as exemplarily shown in Appendix A.1 for the example in Section 3.3. Alternatively, a bounded distribution can be approximated by a continuous distribution, as exemplarily shown Appendix A.2 for the example in Section 3.3. The gradient obtained by this alternative approach however turned out to be very sensitive to the choice of the approximation parameters used therein.

2.3 Taylor series based approximation

Using a Taylor series based approach, the objective function g is approximated by a Taylor series and inserted into Eq. (2) and (3) as, for instance, in [3,18]. Using a first-order approximation is referred to as first-order second-moment method, which yields

$$\begin{aligned} \mu_g(\mathbf{y}) &\approx g(\boldsymbol{\mu}_x,\mathbf{y}) \\ \sigma_g^2(\mathbf{y}) &\approx \sum_{i=1}^{n}\sum_{j=1}^{n} \frac{\partial g(\boldsymbol{\mu}_x,\mathbf{y})}{\partial x_i} \frac{\partial g(\boldsymbol{\mu}_x,\mathbf{y})}{\partial x_j} \mathrm{cov}(X_i,X_j) \end{aligned}$$

Here, $g(\boldsymbol{\mu}_x,\mathbf{y})$ is the objective function evaluated for the mean vector $\boldsymbol{\mu}_x$ of $\mathbf{X}$, and $\frac{\partial g(\boldsymbol{\mu}_x,\mathbf{y})}{\partial x_i}$ is the derivative of g, evaluated at $\boldsymbol{\mu}_x$. The derivatives of the mean and variance approximations are given by

$$\frac{\partial \mu_g(\mathbf{y})}{\partial y_k} \approx \frac{\partial g(\boldsymbol{\mu}_x,\mathbf{y})}{\partial y_k} + \frac{\partial g(\boldsymbol{\mu}_x,\mathbf{y})}{\partial \boldsymbol{\mu}_x} \frac{\partial \boldsymbol{\mu}_x}{\partial y_k} \tag{13}$$

and

$$\begin{aligned} \frac{\partial \sigma_g^2(\mathbf{y})}{\partial y_k} \approx\ & 2\sum_{i=1}^{n}\sum_{j=1}^{n} \frac{\partial^2 g(\boldsymbol{\mu}_x,\mathbf{y})}{\partial x_i \partial y_k} \frac{\partial g(\boldsymbol{\mu}_x,\mathbf{y})}{\partial x_j} \mathrm{cov}(X_i,X_j) \\ & + 2\sum_{i=1}^{n}\sum_{j=1}^{n} \frac{\partial^2 g(\boldsymbol{\mu}_x,\mathbf{y})}{\partial x_i \partial \boldsymbol{\mu}_x} \frac{\partial \boldsymbol{\mu}_x}{\partial y_k} \frac{\partial g(\boldsymbol{\mu}_x,\mathbf{y})}{\partial x_j} \mathrm{cov}(X_i,X_j) \\ & + \sum_{i=1}^{n}\sum_{j=1}^{n} \frac{\partial g(\boldsymbol{\mu}_x,\mathbf{y})}{\partial x_i} \frac{\partial g(\boldsymbol{\mu}_x,\mathbf{y})}{\partial x_j} \frac{\partial \mathrm{cov}(X_i,X_j)}{\partial y_k} \end{aligned} \tag{14}$$

Only the first summands of Eq. (13) and (14) occur if the distribution of $\mathbf{X}$ is independent of $\mathbf{y}$. In case the bounds of the input distribution are design-dependent, as discussed in section 2.1.1, no modification is required for the Taylor series based approach.

2.4 Computational cost

Table 1 summarized the additional terms that have to be evaluated for the different approaches when considering design-dependent random input parameters. Neither the Monte Carlo integration nor the Taylor series based FOSM approach require additional function evaluations and derivatives of the objective function g when compared to a robust design optimization with design-independent distributions. One exception is the case of design-dependent distribution bounds when solved with Monte Carlo (see Sections 2.1.1 and 2.2). Due to the larger number of function evaluations required for Monte Carlo simulations, the FOSM approach is in any case faster. However, the FOSM method requires additional derivatives of the objective function compared to deterministic optimization and Monte Carlo, and it is less accurate.

What additionally comes into play for both approaches are derivatives of the probability density for Monte Carlo and derivatives of the stochastic moments for the Taylor

series approach. This also holds for higher-order Taylor series approaches. Determining these derivatives of the input distribution is, of course, case dependent and not necessarily possible. In order to better demonstrate what information is required for such an optimization, the approaches are applied to examples in Section 3.

Table 1 Overview of terms additionally to be determined for RDO with design-dependent distributions of random variables compared to RDO with constant distributions

	General	Monte Carlo	FOSM
$\frac{\partial \mu_g}{\partial y_k}$	$\int_{-\infty}^{\infty} g \frac{\partial f_{\mathbf{X}}}{\partial y_k} d\mathbf{x}$	$g\left(\mathbf{x}^{(i)}\right)\varphi\left(\mathbf{x}^{(i)}\right)+?^*$	$\frac{\partial g}{\partial \boldsymbol{\mu}_x}\frac{\partial \boldsymbol{\mu}_x}{\partial y_k}$
	eq. (4)	eq. (11)	eq. (13)
$\frac{\partial \sigma_g^2}{\partial y_k}$	$\int_{-\infty}^{\infty} g^2 \frac{\partial f_{\mathbf{X}}}{\partial y_k} d\mathbf{x}$	$g^2\left(\mathbf{x}^{(i)}\right)\varphi\left(\mathbf{x}^{(i)}\right)+?^*$	$\frac{\partial^2 g}{\partial x_i \partial \boldsymbol{\mu}_x}\frac{\partial \boldsymbol{\mu}_x}{\partial y_k}$
	eq. (5)	eq. (12)	eq. (14)

*for bounded distributions, additional sampling on the domain boundary is required, which causes case-dependent additional effort

3 Examples and results

In this section, the approaches discussed in Section 2 are applied to three use cases. For all cases, the objective function is the compliance and in the first section, all derivatives that are required for this objective function are summarized. The use cases have been chosen such that they cover a random load (Section 3.2), random stiffness properties (Section 3.3), and a higher-dimensional problem (Section 3.4). Furthermore, the case of unbounded and bounded stochastic distributions are covered.

3.1 Application to compliance problems using the finite element method

A typical objective function in optimization problems is the compliance $c = \mathbf{u}^T\mathbf{f}$ of a structure where the displacement vector $\mathbf{u}$ is obtained from the equilibrium $\mathbf{K}\mathbf{u} = \mathbf{f}$ with the load vector $\mathbf{f}$ and the symmetric stiffness matrix $\mathbf{K}$.

In the following, it is assumed that the design variables deterministically affect the stiffness and, therefore, implicitly affect the displacements but not the loads. Then, the derivative of the compliance, with respect to a design variable y_k, is given by

$$\frac{\partial c}{\partial y_k} = -\mathbf{u}^T \frac{\partial \mathbf{K}}{\partial y_k}\mathbf{u}$$

The Monte Carlo approach does not required other derivatives. The additional derivatives required for the Taylor series based approach are given in the following subsections where two different cases are distinguished.

3.1.1 Stiffness depending on random parameters

Consider the case that the random parameters X_i affect the stiffness but not the load. Then, the derivatives of the compliance with respect to x_i which are required for the Taylor series approach, are given by

$$\frac{\partial^2 c}{\partial x_i \partial x_j} = -2\mathbf{u}^T \frac{\partial \mathbf{K}}{\partial x_i}\frac{\partial \mathbf{u}}{\partial x_j} - \mathbf{u}^T \frac{\partial^2 \mathbf{K}}{\partial x_i \partial x_j}\mathbf{u}$$

and

$$\frac{\partial^2 c}{\partial x_i \partial y_k} = -2\mathbf{u}^T \frac{\partial \mathbf{K}}{\partial y_k}\frac{\partial \mathbf{u}}{\partial x_i} - \mathbf{u}^T \frac{\partial^2 \mathbf{K}}{\partial x_i \partial y_k}\mathbf{u}$$

The derivatives of the displacement vector $\mathbf{u}$ are obtained from solving

$$\mathbf{K}\frac{\partial \mathbf{u}}{\partial x_i} = -\frac{\partial \mathbf{K}}{\partial x_i}\mathbf{u} \tag{15}$$

Hence, the number of systems (15) to be solved equals the number of random parameters (where the decomposed matrix can be reused as only the right hand side changes). When using the first-order second-moment method for compliance based RDO, the required number of systems to be solved can be reduced to one by use of the adjoint method [12]. For those objective functions where this is not possible, or when using a higher-order approach, the number of random parameters can be reduced by using principal component analysis (also referred to as discrete Karhunen-Loève transform), as, for instance, in [14].

3.1.2 Random load parameters

Consider the case that the random parameters X_i affect the load but not the stiffness. Then, the derivatives of the compliance, with respect to x_i, are given by

$$\frac{\partial c}{\partial x_i} = \frac{\partial c}{\partial f_i} = 2u_i$$

$$\frac{\partial^2 c}{\partial x_i x_j} = \frac{\partial^2 c}{\partial f_i f_j} = 2\frac{\partial u_i}{\partial f_j} \tag{16}$$

and

$$\frac{\partial^2 c}{\partial x_i \partial y_k} = \frac{\partial^2 c}{\partial f_i \partial y_k} = 2\frac{\partial u_i}{\partial y_k} \tag{17}$$

Eq. (16) requires solving

$$\mathbf{K}\frac{\partial \mathbf{u}}{\partial f_j} = \mathbf{e}_j$$

once for each random entry of the load vector and eq. (17) requires solving

$$\mathbf{K}\frac{\partial \mathbf{u}}{\partial y_k} = -\frac{\partial \mathbf{K}}{\partial y_k}\mathbf{u}$$

once for each design parameter.

3.2 Two-bar bracket optimization with random load

A simple truss model, similar to the one discussed in [23], is considered and is shown in Figure 1. The design variable is the angle α and the random parameter is the horizontal force P_h. The length and the cross section of the bars are kept constant with $L = 50$ and $A = 1$, the Young's modulus equals $E = 1000$, and the vertical load is $P_v = 10$.

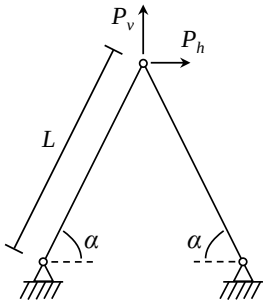

Fig. 1 Two-bar bracket example

In order to use the derivatives given in the previous section 3.1.2, the model is solved using finite elements. The derivative of one element stiffness matrix $\mathbf{K}_e$, with respect to α, equals

$$\frac{\partial \mathbf{K}_e}{\partial \alpha} = \frac{\partial \mathbf{T}^T}{\partial \alpha}\mathbf{K}_{e,loc}\mathbf{T} + \mathbf{T}^T\mathbf{K}_{e,loc}\frac{\partial \mathbf{T}}{\partial \alpha}$$

where $\mathbf{K}_{e,loc}$ is the truss element stiffness matrix in local coordinates and $\mathbf{T}$ is the transformation matrix.

The optimization problem to be solved reads

$$\min_{\alpha} \mu_c(\alpha) + \kappa\,\sigma_c(\alpha)$$

subject to

$$0 \le \alpha \le \pi/2$$
$$\mathbf{K}\,\mathbf{u} = \mathbf{f}$$

The volume/mass of the bracket is implicitly kept constant. Here, a weight factor of $\kappa = 3$ is chosen. In general, the choice of κ is arbitrary and depends on the how the reduction of variability is weighted. It is noted that when assuming the compliance to follow the Gauss distribution, the expression $\mu_c + 3\sigma_c$ corresponds to a compliance that is exceeded with a probability of 0.13%.

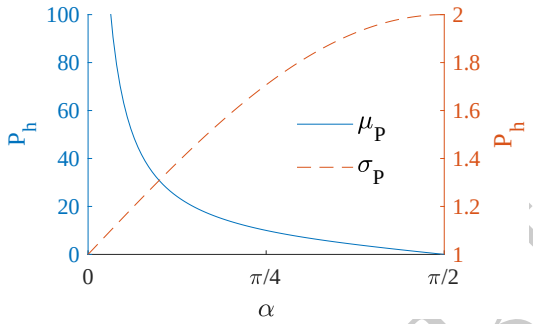

Fig. 2 Mean and standard deviation of the horizontal load as function of the design parameter α

The RDO approach can therefore be considered as a minimization of the 99.87% quantile of the compliance.

The horizontal load P_h is assumed to be Gaussian distributed with mean and standard deviation μ_P and σ_P as functions of α.

$$\begin{aligned}\mu_P &= \frac{10}{\tan\alpha} \\ \sigma_P &= (1+\sin\alpha)\end{aligned} \tag{18}$$

Thereby, for the mean value the resultant of the load components is always aligned with the left bar. The standard deviation is chosen such that it increases as the angle decreases. The functions are shown in Figure 2. The PDF of the horizontal load P_h is then given by

$$f_P(p_h,\alpha) = \frac{1}{\sqrt{2\pi}\sigma_P}\exp\left\{-\tfrac{1}{2}\left(\frac{p_h-\mu_P}{\sigma_P}\right)^2\right\}$$

and the derivative of the PDF, with respect to the design variable α, reads

$$\begin{aligned}\frac{\partial f_P}{\partial \alpha} = &-\frac{1}{\sqrt{2\pi}\sigma_P^2}\frac{\partial \sigma_P}{\partial \alpha}\exp\left\{-\tfrac{1}{2}\left(\frac{p_h-\mu_P}{\sigma_P}\right)^2\right\} \\ &-\frac{1}{\sqrt{2\pi}\sigma_P}\exp\left\{-\tfrac{1}{2}\left(\frac{p_h-\mu_h}{\sigma_h}\right)^2\right\} \\ &\frac{p_h-\mu_P}{\sigma_P}\,\frac{-\frac{\partial \mu_P}{\partial \alpha}\sigma_P - (p_h-\mu_P)\frac{\partial \sigma_P}{\partial \alpha}}{\sigma_P^2}\end{aligned}$$

Since the horizontal load is considered as random parameter P_h, its realization is denoted p_h.

The angle of $\alpha_{ini} = 50^{\circ}$ is considered as the initial design, which is used as start value for the optimizations. The deterministic optimization yields a compliance of 8.4 for an optimal angle of $\alpha_{opt} = 47.5^{\circ}$, where the mean compliance is somewhat higher (see Table 2). The obtained design is analyzed with the FOSM and the Monte Carlo method, using the mean and standard deviation obtained from Eq. (18) with α_{opt}.

When carrying out a robust design optimization with constant, design independent distribution of the random load, a much smaller optimal angle is obtained. For this optimization, the constant mean and variance of P_v are taken from eq. (18) for $\alpha_{ini} = 50^o$. Analyzing the optimized angle with the actual, updated mean and variance of P_v shows that the mean μ_c and the standard deviation σ_c of the compliance were overestimated.

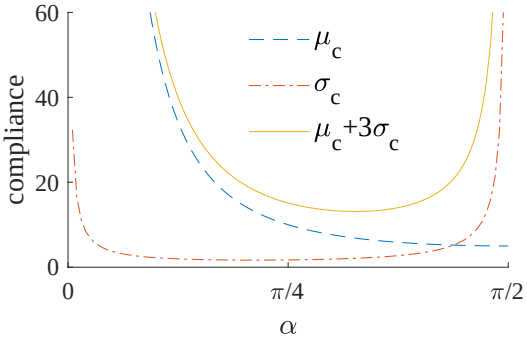

Fig. 3 Mean and standard deviation of the compliance of the two-bar bracket, given by FOSM, as function of the design parameter α

An optimization in which the design dependency of the mean and variance of P_v is taken into account, as discussed in section 2, yields an optimal angle of $\alpha_{opt} = 58.8^o$ when using FOSM and $\alpha_{opt} = 57.2^o$ when using Monte Carlo in the optimization. The mean and standard deviation of the compliance for design dependent random variables are shown in Figure 3 as functions of α.

Table 2 Results of optimizations of the two-bar bracket example

		FOSM		Monte Carlo	
Approach	α_{opt}	μ_c	σ_c	μ_c	σ_c
Deterministic optimization	47.5°	9.2	1.74	9.4	1.75
RDO/FOSM, constant f_P	41.7°	8.8	1.33	9.0	1.34
evaluated with actual f_P		11.3	1.68	11.4	1.69
RDO/FOSM, varying f_P	58.8°	6.8	2.09	7.2	2.14
RDO/MC, varying f_P	57.2°	7.1	2.02	7.4	2.07

For all optimized designs, both the FOSM and the Monte Carlo method yield similar mean values and standard deviations (cf. Table 2), but the computational cost is much lower using FOSM. The Monte Carlo analyses were carried out with 10^5 realizations. A typical measure for the accuracy of a Monte Carlo simulation is the coefficient of variation CoV of the estimates. The equations for determining the CoV of mean value and variance are summarized in Appendix A.3. Using 10^5 samples CoV of mean and variance equal $CoV_{mean} = 0.1\%$ and $CoV_{var} = 0.5\%$ at the end of the optimization. Depending on the desired accuracy, the Monte Carlo simulation could be run with less simulation, decreasing the computational cost. Further efficiency could be gained by using importance sampling or surrogate models. Still, the number of function evaluation would be significantly higher compared to the Taylor series based approach.

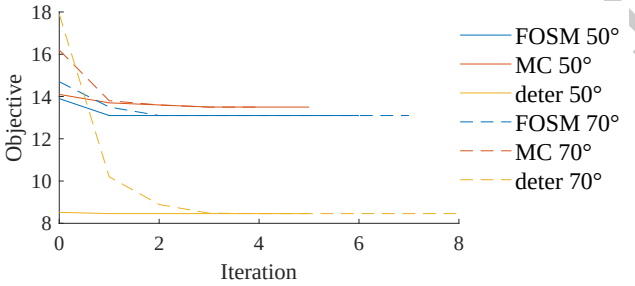

Fig. 4 Objective value over the number of iterations for the two-bar bracket example for different approaches and different start values of α

Figure 4 shows that the RDOs with Monte Carlo and FOSM converge as quickly as the deterministic optimization for different start parameters of $\alpha_0 = 50^o$ and $\alpha_0 = 70^o$. For the RDO with Monte Carlo, new realizations have been generated in each iteration. For a smooth convergence and higher efficiency it is recommended to use the same realizations in all iterations. A smooth convergence should however also be given if the number of realization is large and if the gradient is determined properly, which has been tested with this example. Further RDOs have been carried out in which the distribution of input parameters is updated in each iteration according to Eq. (18), but the design dependency of the distribution is not taken into account in the gradient. These optimizations stopped after a few steps and the results of this specific setting depend heavily on the start value and in some cases do not lead to convergence. This shows the importance of using the correct gradient even for this simple example.

This simple examples, of course, does not allow any general conclusions to be made, but does it show that the design dependency of input distributions can have an impact on the optimal design and that the FOSM approach can be sufficiently accurate.

3.3 Three-bar truss optimization with random cross sections

The next example is the three-bar truss shown in Figure 5, which is similar to an example from [16]. Here, the cross section of each bar is considered as both a design

variable and a random parameter. All other measures are kept constant with $H = 40$, $B = 30$, the Young's modulus equals $E = 1000$, and the vertical and horizontal load equal $P_v = 10$ and $P_h = 1$, respectively.

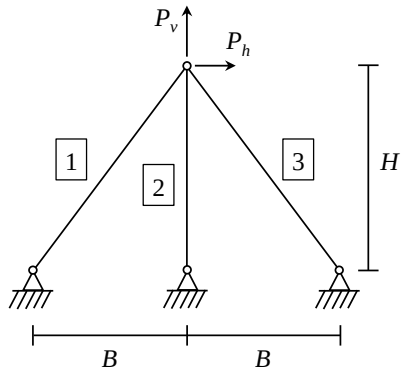

Fig. 5 Three-bar truss example

Since design variables and random parameters refer to the same physical property (namely the cross section a_k), the cross section is split into the nominal cross section $\bar{a}_k$, which is the design variable, and the scattering part $\tilde{a}_k$, which is the random parameter.

$$a_k = \bar{a}_k + \tilde{a}_k$$

The index k refers to the bar. The optimization objective is to minimize the compliance with the constraint that the sum of cross sections is kept constant to a value of 3.0. A weight factor of $\kappa = 5$ is chosen, in order to obtain significantly different results for this example.

$$\min_{\bar{\boldsymbol{a}}} \mu_c + \kappa\, \sigma_c$$

subject to

$$\bar{a}_1 + \bar{a}_2 + \bar{a}_3 = 3.0$$

$$0 \leq \bar{a}_k \leq 1$$

$$\mathbf{K}\,\mathbf{u} = \mathbf{f}$$

The random parameters $\tilde{A}_k$ are chosen to scatter uniformly in the interval $[-0.15\bar{a}_k^2, 0.25\bar{a}_k^2]$. A possible motivation is a manufacturing tolerance for the width and height of a rectangular cross section, which is defined relative to the nominal value. Hence, the interval of the random cross section scales quadratically with the design parameters. The random parameters are assumed to be independently distributed. Based on the chosen interval of the uniform distributions, mean values and standard deviations of each parameter equal

$$\mu_k = 0.05\,\bar{a}_k^2 \quad \text{and} \quad \sigma_k^2 = 0.0133\,\bar{a}_k^4$$

and the derivatives with respect to the design variables are then

$$\frac{\partial \mu_k}{\partial \bar{a}_k} = 0.1\,\bar{a}_k \quad \text{and} \quad \frac{\partial \sigma_k^2}{\partial \bar{a}_k} = 0.0533\,\bar{a}_k^3$$

For optimization with the Monte Carlo method, the PDF either has to be approximated by a continuous function, or the design dependency of integral bounds has to be taken into account as discussed in Section 2.1.1. For the example considered, both possibilities are explained in detail in A.1 and A.2. For the results given in Table 3, the approach considering the design dependency of integral bounds has been used because it turned out to be more robust. It is, however, much more expensive. The number of realizations used within the Monte Carlo simulations equal 10^5 for solving Eqs. (6), (7), (11), and (12). Additionally, 10^5 samples have been generated and evaluated on each face of the cuboid that encloses the domain (see Figure 13).

The deterministic optimization of the truss yields a design in which most material is moved to the central bar (2), while the right bar (3) vanishes (see Table 3). A RDO with constant, design-independent distribution provides almost the same design. When the design dependency of the random distribution is accounted for, the material is distributed more evenly between all bars and the standard deviation of the compliance decreases while the mean compliance increases. Again, carrying out the RDO with the FOSM and the Monte Carlo method results in almost the same design. Figure 6 shows that also for the three-bar truss example the RDOs converge as quickly as the deterministic optimization.

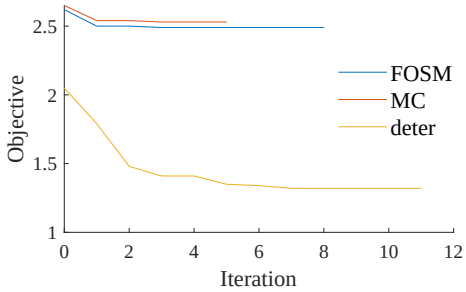

Fig. 6 Objective value over the number of iterations for the three-bar truss example for different approaches

The mean values and standard deviations of the optimized designs obtained by the FOSM and the Monte Carlo method are in good agreement, except for one case. For the result of the RDO with constant input distribution, the FOSM method estimates a standard deviation close to zero, which is wrong according to the Monte Carlo analysis. This phenomenon occurs if the

Table 3 Results of optimizations of the three-bar truss example

	Design parameters			FOSM		Monte Carlo	
Approach	a_1	a_2	a_3	μ_c	σ_c	μ_c	σ_c
Deter. optimization	0.54	2.82	0.0	1.18	0.27	1.28	0.33
RDO/FOSM with constant $f_{\tilde{\mathbf{A}}}$	0.62	2.73	0.0	1.24	0.06	1.27	0.32
evaluated with actual $f_{\tilde{\mathbf{A}}}$				1.19	0.27	1.28	0.33
RDO/FOSM with varying $f_{\tilde{\mathbf{A}}}$	1.10	1.36	0.62	1.69	0.16	1.71	0.17
RDO/MC with varying $f_{\tilde{\mathbf{A}}}$	1.13	1.30	0.63	1.72	0.16	1.74	0.16

objective function has a local minimum with respect to the random parameters as a results of a RDO (see, e.g., [12]).

3.4 Topology optimization with random Young's moduli

The last example is a robust topology optimization using the Simplified Isotropic Material with Penalization (SIMP) approach [4]. Each design variable ρ_e is associated with one finite element of the design space. The optimization problem reads

$$\min_{\boldsymbol{\rho}} \mu_c(\boldsymbol{\rho}) + \kappa\, \sigma_c(\boldsymbol{\rho})$$

subject to

$$\frac{V(\boldsymbol{\rho})}{V_0} \leq v$$

$$0 \leq \rho_e \leq 1$$

$$\mathbf{K}\,\mathbf{u} = \mathbf{f}$$

A weight factor of $\kappa = 5$ is chosen. The design variables ρ_e are filtered and projected using the same approach as, for instance, in [26]. Further details are summarized in A.4.

The random parameters considered are the Young's moduli E_k in each element. They are considered to be spatially correlated, according to the Gaussian correlation function, with a correlation length l_c. The correlation r_{ij} of two Young's moduli E_i and E_j is assumed to be independent of the design and so is the mean value μ_E, but the standard deviation of each element is considered as design-dependent. Hence, the covariance of the Young's moduli is design-dependent according to

$$\mathrm{cov}(E_i, E_j) = r_{ij} \cdot \sigma_i(\boldsymbol{\rho}) \cdot \sigma_j(\boldsymbol{\rho})$$

Hence, the derivative of the covariance equals

$$\frac{\partial \mathrm{cov}(E_i, E_j)}{\partial \rho_k} = r_{ij}\left[\frac{\partial \sigma_i}{\partial \rho_k}\sigma_j + \sigma_i \frac{\partial \sigma_j}{\partial \rho_k}\right]$$

The standard deviation of the Young's modulus in each element is assumed to be dependent on the design parameters in the below elements. A motivation could be that in an additive manufacturing process the material properties in supported areas are better than those in overhang area. Undoubtedly, this is a very complex phenomenon and its realistic simulation is outside the scope of this paper. Here, a very simple model is used in which for each element the *supporting neighbors* are determined. As shown in Figure 7, the supporting neighbors are the elements below the considered element that are in a certain range and within a certain angle. The number of supporting neighbors of the j-th element is denoted $n_{N,j}$ and the indices of the supporting neighbors are summarized in Q_j. The degree of filling $v_{N,j}$ of the neighborhood is defined as

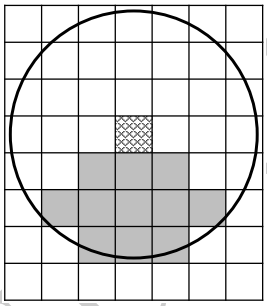

Fig. 7 Supporting neighbors (gray) of one element (hatched) within a defined range (black circle)

$$v_{N,j} = \frac{\sum\limits_{i \in Q_j} \rho_i}{n_{N,j}} \quad \text{with} \quad n_{N,j} = \sum_{i \in Q_j} i$$

The standard deviation of E_j is defined as a function of $v_{N,j}$ by

$$\sigma_j = \sigma_0 (1 - v_{N,j})^2 \tag{19}$$

Thereby, the σ_j equals zero if all supporting elements are filled, and σ_j equals σ_0 if all supporting elements are empty. The derivative of the standard deviation, which is required to determine the derivative of the covariances, is given by

$$\frac{\partial \sigma_j}{\partial \rho_k} = \begin{cases} -2\dfrac{\sigma_0}{n_{N,j}}(1 - v_{N,j}) & \text{if } k \in Q_j \\ 0 & \text{else} \end{cases}$$

The determination of supporting neighbors is inspired by the overhang detection used in the approach by Langelaar [13].

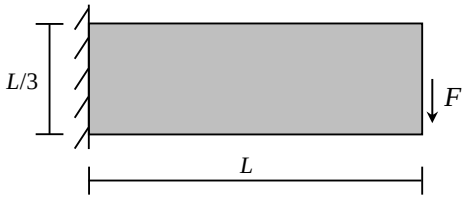

Fig. 8 Design space of topology optimization example

The design space, load application, and boundary conditions of the example considered are shown in Figure 8. The optimization was stopped after 150 iterations. The standard deviation factor of $\sigma_0 = 7.5$ is chosen. For the optimizations with design-independent distributions, a fixed standard deviation of $\sigma_E = 1.5$ is used. A correlation length of $l_c = 9.6$ is chosen and the radius in which supporting neighbors are determined equals 13. Further settings of the topology optimization are summarized in Table 4.

Table 4 Properties of the topology optimization example

Design space size	$L = 90$
Element edge length	$L_e = 1$
Applied load	$F = 1$
Volume fraction	$V/V_0 = 50\%$
Filter radius	$R = 3.6$
Material properties	$E = 10$, $\nu = 0.3$
Projection parameters	$\eta = 0.5$, $\beta = 10$

For the robust topology optimization, the FOSM based approach given in [12] is used. There, the gradient of the variance is obtained by solving one adjoint system per iteration. The gradient of the variance given in [12] equals the first term of Eq. (14). The additional terms originating from the design dependency of the random variables are simply added. For the given example, the second term in Eq. (14) equals zero and only the last term needs to be evaluated. For the current example this term reads

$$\sum_{i=1}^{n}\sum_{j=1}^{n}\frac{\partial c}{\partial E_i}\frac{\partial c}{\partial E_j}\frac{\partial \mathrm{cov}(E_i,E_j)}{\partial \rho_k}$$

where n is the number of elements. This term does not require additional FE calculations or solutions of adjoint systems. However, the author found that updating the derivative of the covariance matrix can be a computationally expensive procedure. The reason is that covariance matrix is, in general, a full matrix of the size $n \times n$, and the same holds for its derivative, which has to be setup n times.

Table 5 Results of optimizations of the three-bar truss example

	FOSM		Monte Carlo	
Approach	μ_c	σ_c	μ_c	σ_c
Deter. optimization	18.0	1.38	19.5	2.40
RDO with constant $f_{\mathbf{E}}$	18.0	0.82		
evaluated with actual $f_{\mathbf{E}}$	18.0	1.35	19.6	2.40
RDO with varying $f_{\mathbf{E}}$	19.1	0.72	20.0	1.23

The result of a deterministic topology optimization is shown in Figure 9. The mean value and standard deviation of the compliance of the final design is given in Table 5. A robust topology optimization with constant, design-independent input distribution yields almost the same topology and is, therefore, not shown; although, the standard deviation is further reduced compared to the deterministic optimization.

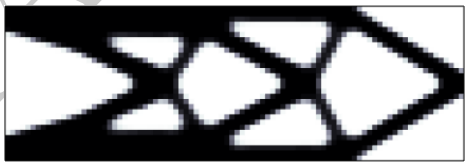

Fig. 9 Result of the deterministic topology optimization

The mean and standard deviation are determined with the FOSM method within the optimization process and validated the Monte Carlo method for the final design. The Monte Carlo simulation results show that the compliance is highly skewed with extreme outliers. Therefore, the robust estimators given in [22] are used, which is available in Matlab. The Monte Carlo estimates significantly differ from the FOSM result. The tendency, however, remains the same.

Fig. 10 Result of the robust topology optimization with design-dependent distribution of Young's moduli

The result of the RTO with design-dependent covariance shown in Figure 10 significantly differs from the deterministic result and lead to a lower standard

deviation of the compliance. The cause of the decreased standard deviation of the compliance is clear when Figures 11 and 12 are compared. The plots show the standard deviation of the Young's modulus in each element for the final designs from deterministic optimization and RTO. Due to the material-free area at the left boundary of the design space, the standard deviation of Young's moduli is high in the upper left corner. Therefore, the upper beam of the deterministic design experiences large scatter. The RTO that considers the design dependency of input parameters provides a design with increased thickness in this area, which decreases the area of the upper beam with a large scatter of Young's moduli.

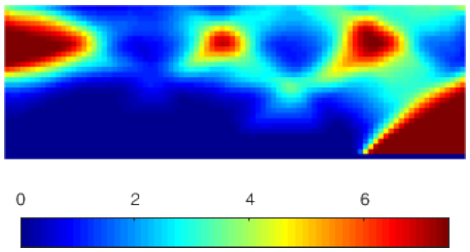

Fig. 11 Standard deviations of Young's moduli for the deterministically optimized design

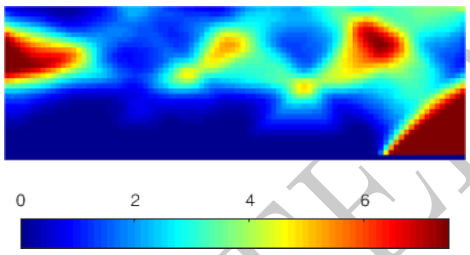

Fig. 12 Standard deviations of Young's moduli for the design obtained from robust topology optimization with design-dependent distribution of Young's moduli

4 Conclusions and outlook

This paper presents a theory for incorporating design dependency of random variables in the gradient of the robust design optimization. Approaches to determine the gradient with Taylor series approximations and with Monte Carlo simulations are shown. The application of these approaches is demonstrated with simple examples that show the impact of neglecting the effect of the design dependency of input distributions and what additional information is required for considering the design dependency.

The implications of considering bounded stochastic distributions is discussed. This issue is expected to become much more challenging for high-dimensional distributions and/or distributions with correlated variables.

For the presented examples, the dependence of the input distributions is chosen. For real applications, deriving this relationship (and its derivative) is the major challenge of applying the method and will be subject of future research. This could be achieved by using process simulation to determine the stochastic distribution of input parameters. These process simulations have to be very efficient since they need to be embedded in an optimization, and their result must be differentiable with respect to design parameters, which is a major challenge.

The current paper deals uncertainties in a probabilistic sense. However, there are alternative approaches for uncertainty propagation, like interval analyses, convex set theory or Fuzzy logic [7], as well as hybrid approaches combining both (see, e.g., [33,10]). Each approach can be used for design optimization under uncertainty (e.g., [9,30]) and of course, for each approach the gradients to be computed are different. Hence, considering design-dependent description of uncertain input parameters requires further derivations for these methods.

A Appendix

A.1 Derivative of 3D uniform distribution

Consider an objective function g as function of three design parameters $\mathbf{y} = (y_1, y_2, y_3)^T$ and three random parameters $\mathbf{X} = (X_1, X_2, X_3)^T$. The random parameters are considered to be independent, hence their joint PDF reads

$$f_{\mathbf{X}} = f_{X_1} \cdot f_{X_2} \cdot f_{X_3}$$

The individual PDFs are given by

$$f_{X_i} = \begin{cases} \dfrac{1}{u_i - l_i} & l_i \le x_i \le u_i \\ 0 & \text{else} \end{cases}$$

where each interval bound is a function of one design parameter, i.e. $u_i(y_i), l_i(y_i)$. The derivative of the mean of the objective function μ_g, with respect to the first design variable

y_1, is then given by

$$\begin{aligned}\frac{\partial \mu_g}{\partial y_1} &= \frac{\partial}{\partial y_1}\int_{l_1}^{u_1}\int_{l_2}^{u_2}\int_{l_3}^{u_3} g\left(\mathbf{x},\mathbf{y}\right) f_{\mathbf{X}} dx_3 dx_2 dx_1 \\ &= \int_{l_1}^{u_1}\int_{l_2}^{u_2}\int_{l_3}^{u_3} \frac{\partial g}{\partial y_1} f_{\mathbf{X}} dx_3 dx_2 dx_1 + \int_{l_1}^{u_1}\int_{l_2}^{u_2}\int_{l_3}^{u_3} g \frac{\partial f_{\mathbf{X}}}{\partial y_1} dx_3 dx_2 dx_1 \\ &+ \frac{\partial u_1}{\partial y_1} f_{X_1}\left(u_1\right) \int_{l_2}^{u_2}\int_{l_3}^{u_3} g\left(u_1, x_2, x_3, \mathbf{y}\right) f_{X_2} f_{X_3} dx_3 dx_2 \\ &- \frac{\partial l_1}{\partial y_1} f_{X_1}\left(l_1\right) \int_{l_2}^{u_2}\int_{l_3}^{u_3} g\left(l_1, x_2, x_3, \mathbf{y}\right) f_{X_2} f_{X_3} dx_3 dx_2\end{aligned} \tag{20}$$

The first two terms can be determined by the Monte Carlo method as given by Eq. (11) and (12). The latter two terms need to be solved by generating samples on the surface of the cuboid shown in Figure 13, which represents the domain of $\mathbf{X}$. The Monte Carlo approximation of the third term of Eq. (20) equals

$$\int_{l_2}^{u_2}\int_{l_3}^{u_3} g\left(u_1, x_2, x_3, \mathbf{y}\right) f_{X_2} f_{X_3} dx_3 dx_2 \approx \frac{1}{m}\sum_{i=1}^{m} g\left(u_1, x_2^{(i)}, x_3^{(i)}, \mathbf{y}\right)$$

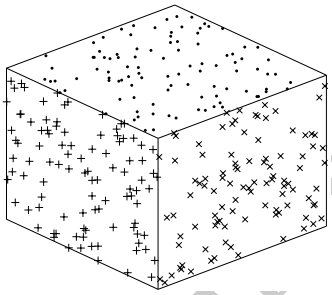

Fig. 13 Example of samples generated on the faces of a cuboid

The approximation of the fourth term is similar. The derivatives, with respect to y_2 and y_3, are obtained in the same manner. Also, the derivative of the variance is determined the same way as only the objective function needs to be squared.

A.2 Continuous approximation of uniform distribution

Instead of considering the design dependency of the domain by the integral bounds, a non-continuous function can be approximated by a continuous one. Then, the Monte Carlo approximations (6) to (12) can be solved as given before. This is exemplarily shown for the uniform distribution. A uniform distribution in the interval $[a, b]$ can be approximated by

$$f_X\left(x\right) = \left\{\begin{array}{ll}\dfrac{1}{b-a} & a \le x \le b \\ 0 & \text{else}\end{array}\right\} \approx h_L \cdot f_C \cdot h_R \tag{21}$$

with

$$f_C = \frac{1}{b-a}, \quad h_L = 0.5 + 0.5\tanh\left(k\left(x-a\right)\right)$$
$$\text{and} \quad h_R = 0.5 + 0.5\tanh\left(k\left(b-x\right)\right)$$

The factor k defines how close h_L and h_R approximate the Heaviside function. The approximation and its factors are visualized in Figure 14 and 15.

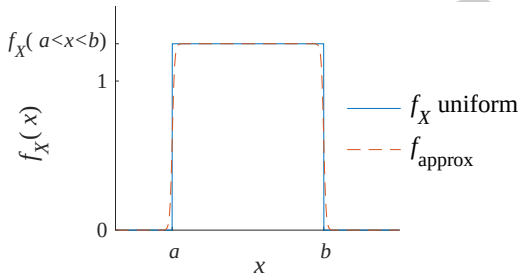

Fig. 14 Uniform distribution and continuous approximation

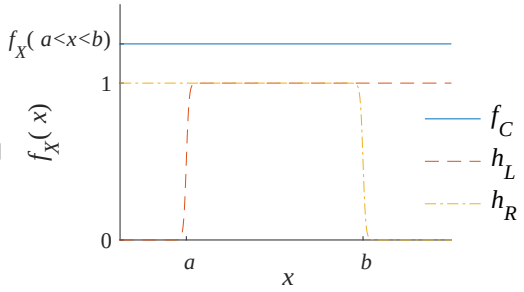

Fig. 15 Factors of the continuous approximation of uniform distribution

The derivative of the uniform distribution, with respect to the bounds a and b, is then approximated by

$$\begin{aligned}\frac{\partial f_X\left(x\right)}{\partial a} &\approx \frac{\partial h_L}{\partial a}\cdot f_C \cdot h_R + h_L \cdot \frac{\partial f_C}{\partial a}\cdot h_R \\ \frac{\partial f_X\left(x\right)}{\partial b} &\approx h_L \cdot \frac{\partial f_C}{\partial b}\cdot h_R + h_L \cdot f_C \cdot \frac{\partial h_R}{\partial b}\end{aligned} \tag{22}$$

with

$$\frac{\partial f_C}{\partial a} = \frac{1}{\left(b-a\right)^2} \qquad \frac{\partial h_L}{\partial a} = -0.5\text{sech}^2\left(k\left(x-a\right)\right)k$$
$$\frac{\partial f_C}{\partial b} = -\frac{1}{\left(b-a\right)^2} \qquad \frac{\partial h_R}{\partial b} = 0.5\text{sech}^2\left(k\left(b-x\right)\right)k$$

A.3 Coefficient of variation of moment estimators

Given m realizations $x^{(i)}$ of a random vector X (which may be the outcomes of a Monte Carlo simulation), the mean μ_X and variance σ_X^2 are estimated using the estimators $\bar{x}$ and s^2.

$$\mu_X \approx \bar{x} = \frac{1}{m}\sum_{i=1}^{m} x^{(i)} \qquad \sigma_X^2 \approx s^2 = \frac{1}{m-1}\sum_{i=1}^{m}\left(x^{(i)} - \bar{x}\right)^2$$

These estimators are random parameters themselves. The mean and variance of the estimators are given by

$$\mu_{\bar{x}} = \mu_X \qquad \sigma^2_{\bar{x}} = \frac{\sigma^2_X}{m}$$

and

$$\mu_{s^2} = \sigma^2_X \qquad \sigma^2_{s^2} = \frac{1}{m}\left(\mu_{X,4} - \frac{m-3}{m-1}\sigma^4_X\right)$$

A measure for the accuracy of the estimators are their coefficients of variation CoV, which are given by

$$CoV_{\bar{x}} = \frac{\sigma_{\bar{x}}}{\mu_{\bar{x}}} = \frac{\sigma_X}{\mu_X\sqrt{m}}$$

and

$$CoV_{s^2} = \frac{\sigma_{s^2}}{\mu_{s^2}} = \frac{1}{\sigma^2_X}\sqrt{\frac{1}{m}\left(\mu_{X,4} - \frac{m-3}{m-1}\sigma^4_X\right)} = \sqrt{\frac{1}{m}\left(\kappa_X - \frac{m-3}{m-1}\right)}$$

Here, κ_X is the kurtosis of X.

For a detailed derivation of these estimators, see Section 8.2 in [31].

A.4 Details on the topology optimization approach

The design variables ρ_e are filtered and projected using the same approach as in [26]. The filter function and its derivative equal

$$\tilde{\rho}_e = \frac{\sum_{i=1}^{Q} w_{ei} v_i \rho_i}{\sum_{i=1}^{Q} w_{ei} v_i} \quad \text{and} \quad \frac{\partial \tilde{\rho}_e}{\partial \rho_k} = \frac{w_{ek} v_k}{\sum_{i=1}^{Q} w_{ei} v_i}$$

with $w_{ei} = \max(0, R - r_{ei})$. Here, v_i is the volume of the i-th element, r_{ei} is the distance of the i-th element to the e-th element, and R is the filter radius. Q can be the number of elements, but in practical implementation it is the number of neighbor elements.

In each iteration, the filtered design variable $\tilde{\rho}$ is projected to a value of either 0 or 1 in order to avoid elements with intermediate density. This projection is done by an approximation of the Heaviside function proposed by Wang et al. [29].

$$\bar{\tilde{\rho}} = \frac{\tanh(\beta\eta) + \tanh(\beta(\tilde{\rho} - \eta))}{\tanh(\beta\eta) + \tanh(\beta(1 - \eta))}$$

The projected variable $\bar{\tilde{\rho}}$ is used to penalize the stiffness, to determine the volume, and also to determine the standard deviation in in Eq. (19). Hence, the obtained derivatives are actually derivatives with respect to $\bar{\tilde{\rho}}$. The derivative (e.g. of c), with respect to the actual design variable ρ, is obtained by

$$\frac{\partial c}{\partial \rho_k} = \frac{\partial c}{\partial \bar{\tilde{\rho}}_e} \frac{\partial \bar{\tilde{\rho}}_e}{\partial \tilde{\rho}_e} \frac{\partial \tilde{\rho}_e}{\partial \rho_k}$$

B Notes

B.1 Conflict of Interest

The author states that there is no conflict of interest.

B.2 Replication of Results

The author states that the paper contains all information necessary to reproduce the results.

References

1. Arbocz, J.: Past, Present and Future of Shell Stability Analysis. Zeitschrift für Flugwissenschaften und Weltraumforschung **5**(6), 335–348 (1981)
2. Arbocz, J.: Recent developments in shell stability analysis. Journal of Theoretical and Applied Mechanics **25**(4), 523–540 (1987). URL http://www.ptmts.org.pl/jtam/index.php/jtam/article/view/v25n4p523
3. Asadpoure, A., Tootkaboni, M., Guest, J.K.: Robust topology optimization of structures with uncertainties in stiffness – Application to truss structures. Computers & Structures **89**(11), 1131–1141 (2011). DOI 10.1016/j.compstruc.2010.11.004. URL http://www.sciencedirect.com/science/article/pii/S004579491000266X
4. Bendsøe, M.P.: Optimal shape design as a material distribution problem. Structural optimization **1**(4), 193–202 (1989). DOI 10.1007/BF01650949. URL https://link.springer.com/article/10.1007/BF01650949
5. Cho, H., Choi, K.K., Lamb, D.: Sensitivity Developments for RBDO With Dependent Input Variable and Varying Input Standard Deviation. Journal of Mechanical Design **139**(7), 071,402 (2017). DOI 10.1115/1.4036568. URL http://mechanicaldesign.asmedigitalcollection.asme.org/article.aspx?doi
6. Doltsinis, I., Kang, Z.: Robust design of structures using optimization methods. Computer Methods in Applied Mechanics and Engineering **193**(23), 2221–2237 (2004). DOI 10.1016/j.cma.2003.12.055. URL http://www.sciencedirect.com/science/article/pii/S0045782504000787
7. Elishakoff, I.: An Idea of the Uncertainty Triangle. The Shock and Vibration Digest **22**, 1 (1990)
8. Haldar, A., Mahadevan, S.: Probability, Reliability and Statistical Methods in Engineering Design, 1. auflage edn. John Wiley & Sons, New York ; Chichester England (1999)
9. Hu, N., Duan, B.: An efficient robust optimization method with random and interval uncertainties. Structural and Multidisciplinary Optimization **58**(1), 229–243 (2018). DOI 10.1007/s00158-017-1892-0. URL https://link.springer.com/article/10.1007/s00158-017-1892-0
10. Jiang, C., Zheng, J., Han, X.: Probability-interval hybrid uncertainty analysis for structures with both aleatory and epistemic uncertainties: a review. Structural and Multidisciplinary Optimization **57**(6), 2485–2502 (2018). DOI 10.1007/s00158-017-1864-4. URL https://doi.org/10.1007/s00158-017-1864-4
11. Keller, N., Ploshikhin, V.: New method for fast predictions of residual stress and distortion of AM parts. In: Solid Freeform Fabrication Symposium (SFF). Austin, TX (2014)

12. Kriegesmann, B., Lüdeker, J.K.: Robust compliance topology optimization using the first-order second-moment method. Structural and Multidisciplinary Optimization **60**(1), 269–286 (2019). DOI 10.1007/s00158-019-02216-8. URL https://doi.org/10.1007/s00158-019-02216-8
13. Langelaar, M.: An additive manufacturing filter for topology optimization of print-ready designs. Structural and Multidisciplinary Optimization **55**(3), 871–883 (2017). DOI 10.1007/s00158-016-1522-2. URL https://link.springer.com/article/10.1007/s00158-016-1522-2
14. Lazarov, B.S., Schevenels, M., Sigmund, O.: Topology optimization with geometric uncertainties by perturbation techniques. International Journal for Numerical Methods in Engineering **90**(11), 1321–1336 (2012). DOI 10.1002/nme.3361. URL http://onlinelibrary.wiley.com/doi/10.1002/nme.3361/abstract
15. Lee, I., Choi, K.K., Du, L., Gorsich, D.: Dimension reduction method for reliability-based robust design optimization. Computers & Structures **86**(13), 1550–1562 (2008). DOI 10.1016/j.compstruc.2007.05.020. URL http://www.sciencedirect.com/science/article/pii/S0045794907001897
16. Lee, K.H., Park, G.J.: Robust optimization considering tolerances of design variables. Computers & Structures **79**(1), 77–86 (2001). DOI 10.1016/S0045-7949(00)00117-6. URL http://www.sciencedirect.com/science/article/pii/S0045794900001176
17. Liebisch, M., Hein, R., Wille, T.: Probabilistic process simulation to predict process induced distortions of a composite frame. CEAS Aeronautical Journal **9**(4), 545–556 (2018). DOI 10.1007/s13272-018-0302-7. URL http://link.springer.com/10.1007/s13272-018-0302-7
18. Papoutsis-Kiachagias, E.M., Papadimitriou, D.I., Giannakoglou, K.C.: Robust design in aerodynamics using third-order sensitivity analysis based on discrete adjoint. Application to quasi-1d flows. International Journal for Numerical Methods in Fluids **69**(3), 691–709 (2012). DOI 10.1002/fld.2604. URL https://onlinelibrary.wiley.com/doi/abs/10.1002/fld.2604
19. Park, G.J., Lee, T.H., Lee, K.H., Hwang, K.H.: Robust Design: An Overview. AIAA Journal **44**(1), 181–191 (2006). DOI 10.2514/1.13639. URL https://doi.org/10.2514/1.13639
20. Protter, M.H., Morrey, C.B.J.: Intermediate Calculus, 2 edn. Springer, New York (1985)
21. Rahman, S.: Stochastic sensitivity analysis by dimensional decomposition and score functions. Probabilistic Engineering Mechanics **24**(3), 278–287 (2009). DOI 10.1016/j.probengmech.2008.07.004. URL https://linkinghub.elsevier.com/retrieve/pii/S0266892008000635
22. Rousseeuw, P.J., Driessen, K.V.: A Fast Algorithm for the Minimum Covariance Determinant Estimator. Technometrics **41**(3), 212–223 (1999). DOI 10.1080/00401706.1999.10485670
23. Rozvany, G.I.N., Maute, K.: Analytical and numerical solutions for a reliability-based benchmark example. Structural and Multidisciplinary Optimization **43**(6), 745–753 (2011). DOI 10.1007/s00158-011-0637-8. URL https://link.springer.com/article/10.1007/s00158-011-0637-8
24. Rubinstein, R.Y., Shapiro, A.: Discrete event systems: Sensitivity analysis and stochastic optimization by the score function method. John Wiley & Sons (1993)
25. Sandgren, E., Cameron, T.M.: Robust design optimization of structures through consideration of variation. Computers & Structures **80**(20), 1605–1613 (2002). DOI 10.1016/S0045-7949(02)00160-8. URL http://www.sciencedirect.com/science/article/pii/S0045794902001608
26. Schevenels, M., Lazarov, B.S., Sigmund, O.: Robust topology optimization accounting for spatially varying manufacturing errors. Computer Methods in Applied Mechanics and Engineering **200**(49–52), 3613–3627 (2011). DOI 10.1016/j.cma.2011.08.006. URL http://www.sciencedirect.com/science/article/pii/S0045782511002611
27. Schuëller, G.I., Jensen, H.A.: Computational methods in optimization considering uncertainties – An overview. Computer Methods in Applied Mechanics and Engineering **198**(1), 2–13 (2008). DOI 10.1016/j.cma.2008.05.004. URL http://www.sciencedirect.com/science/article/pii/S0045782508002028
28. Sigmund, O.: On the usefulness of non-gradient approaches in topology optimization. Structural and Multidisciplinary Optimization **43**(5), 589–596 (2011). DOI 10.1007/s00158-011-0638-7. URL https://link.springer.com/article/10.1007/s00158-011-0638-7
29. Wang, F., Lazarov, B.S., Sigmund, O.: On projection methods, convergence and robust formulations in topology optimization. Structural and Multidisciplinary Optimization **43**(6), 767–784 (2011). DOI 10.1007/s00158-010-0602-y. URL https://link.springer.com/article/10.1007/s00158-010-0602-y
30. Wang, L., Liang, J., Wu, D.: A non-probabilistic reliability-based topology optimization (NRBTO) method of continuum structures with convex uncertainties. Structural and Multidisciplinary Optimization **58**(6), 2601–2620 (2018). DOI 10.1007/s00158-018-2040-1. URL https://doi.org/10.1007/s00158-018-2040-1
31. Wilks, S.S.: Mathematical statistics. Wiley (1962)
32. Zang, T.A., Hemsch, M.J., Hilburger, M.W., Kenny, S.P., Luckring, J.M., Maghami, P., Padula, S.L., Stroud, W.J.: Needs and opportunities for uncertainty-based multidisciplinary design methods for aerospace vehicles. Tech. Rep. NASA/TM-2002-211462, National Aeronautics and Space Administration, Langley Research Center (2002)
33. Zhang, J., Xiao, M., Gao, L., Fu, J.: A novel projection outline based active learning method and its combination with Kriging metamodel for hybrid reliability analysis with random and interval variables. Computer Methods in Applied Mechanics and Engineering **341**, 32–52 (2018). DOI 10.1016/j.cma.2018.06.032. URL http://www.sciencedirect.com/science/article/pii/S0045782518303293
34. Zhang, T.: Robust reliability-based optimization with a moment method for hydraulic pump sealing design. Structural and Multidisciplinary Optimization **58**(4), 1737–1750 (2018). DOI 10.1007/s00158-018-1996-1. URL https://doi.org/10.1007/s00158-018-1996-1